

Assembly of polyfunctional compounds from the cyanide and isocyanate building blocks through the nanoparticle-catalyzed multicomponent reactions: A review

M. Sarkar^{*,#} and Grigoriy A. Sereda^{*,§}

Department of Chemistry, University of South Dakota, Vermillion, SD 57069, USA.

ABSTRACT

Multicomponent reactions (MCRs) provide a facile one-pot approach to molecules with multiple chiral centers, which reveals a significant potential for the preparation of the libraries of chiral compounds. Utilization of nanoparticles (NPs) to catalyze MCRs further advances their synthetic value and versatility. NPs can be readily separated from reaction mixtures by filtration, centrifugation, or magnet-assisted separation of magnetic nanoparticles. Functionalization of nanoparticles is now widely explored as a powerful tool for the design and fine-tuning of catalytic properties of nanoparticles. This review focuses on the last decade's progress in the utilization of the reversely polarized C-N bonds of cyanides and isocyanides as the versatile building units of a variety of heterocyclic and pharmaceutically relevant linear organic compounds.

KEYWORDS: multicomponent reaction, cyanide, isocyanide, nanoparticles, catalysis.

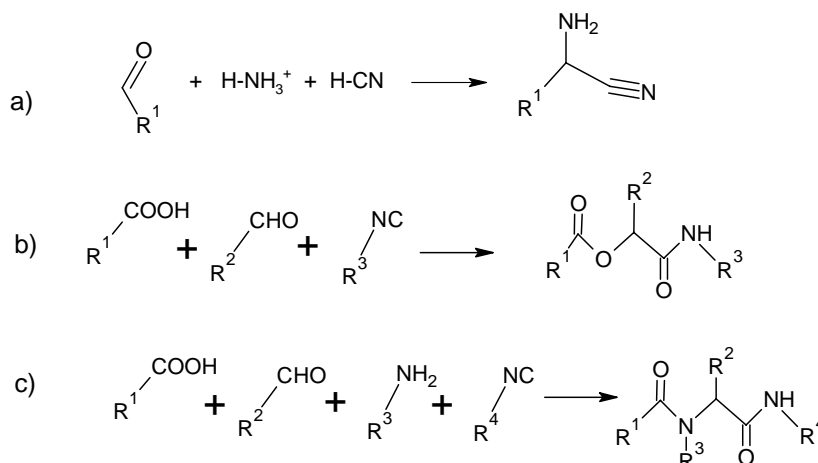
1. Introduction

Multicomponent organic reactions (MCRs) involve more than two starting reactants in a reaction to produce a single product [1, 2]. The structure of the desired product can be easily varied by using different derivatives of the reactant [1]. MCRs have been known for over more than 160 years since 1850 when Strecker first reported the synthesis of

α -aminocyanides from ammonia, carbonyl compounds and hydrogen cyanide (Scheme 1a) [3]. MCRs have provided access to the products with a variety of industrial applications. Over the last few decades, chemists around the world have been focusing on multicomponent reactions in drug development as products obtained from MCRs have significant molecular diversity, can be synthesized faster, and they have high dispersion rates through the organ system [4, 5]. The high molecular diversity of the MCR products is achieved through the rapid building of multiple bonds in a one-pot, single-step reaction resulting in minimal waste and requiring less energy than building the target structure bond-by-bond [6, 7]. Thus not surprisingly, MCRs are widely used for the rapid assembly of bioactive compounds. The classification of MCRs includes the reaction types and the nature of the reactants [8]. There are three generally accepted MCR types: a) Type I consists of MCRs where an equilibrium is maintained among reactants, intermediates and final products; b) In the MRCs of Type II, the equilibrated system of the reactants and intermediates produces the target in an irreversible process; c) A Type III MCR is a sequence of practically irreversible steps from reactants to products [9]. In 1921, Passerini (Scheme 1b) first introduced an isocyanide-based three-component reaction [10] while Ugi in 1959 put forward a four-component reaction also involving an isocyanide [11] (Scheme 1c). The widespread use of isocyanides in MCRs is accounted for their ability to sequentially react with electrophiles and nucleophiles which eventually forms α -adducts [12]. However, isocyanides are

*Corresponding authors

[§]grigoriy.sereda@usd.edu; [#]akash.mamon@gmail.com



Scheme 1. a) Preparation of α -aminocyanides by Strecker; b) Passerini 3RC; c) Ugi 4RC.

toxic and produce a noticeable stench [13, 14]. In 1882, Hantzsch developed another versatile MCR producing dihydropyrimidine from aldehyde, amine and β -keto ester [15].

MCRs allow us to simultaneously generate multiple chiral centers which can be used for the preparation of chiral compound libraries [12]. Stereoisomers usually have different biological activity relevant to agriculture [16] and pharmaceutical industries [17] which further expands the practical applications of MCRs. MCRs are considered to be more convenient over linear synthesis as the latter involves several steps with progressively decreasing overall yield [18]. An additional benefit of MCRs is their high atom economy, since a significant fraction of atoms in the reactants is retained in the final product [19].

Different homogeneous and heterogeneous catalysts have been used to improve the reaction rate, yield and selectivity. However, some catalytic systems are hazardous as they involve toxic transition metals [20-22] and hazardous solvents [23-25]. Researchers all over the world have been continuously looking for ecofriendly and cost-effective catalysts. Homogeneous catalysts used in industrial applications could be costly and hard to fully recover from the reaction mixture and reuse [26]. Besides, it is especially important to remove traces of the catalyst from a pharmaceutical final product. Therefore, researchers are interested in heterogeneous catalysts. Heterogeneous catalysts are usually reusable for many times with minimal loss of

reactivity, which is a welcome characteristic from an ecofriendly and sustainable green chemistry perspective. However, heterogeneous catalysts are often less effective than the homogeneous catalysts [27] due to the surface area and the reagent flow dynamics limitations.

At the beginning of the new millennium, the world witnessed an extensive use of nanoparticles (NPs) in very diverse areas of research. Due to the higher surface area and often a different surface energy and chemistry, NPs often show superior catalytic activity compared to bulk materials [28, 29]. NPs with a large surface area, presence of cavities on the surface, and stability at elevated temperatures have been widely explored as potential catalysts for various organic reactions [30, 31]. A spherical 10 nm nanoparticle exposes $600 \text{ m}^2/\text{cm}^3$ of the surface area and is more accessible compared to a bulk heterogeneous catalyst [27]. A nanomaterial can be defined as a material with at least one dimension no more than 100 nm. It can be made of metals, metal oxides, organometallics, ceramics, polymers, composite, and other materials. NPs are also considered as a more sustainable catalyst than conventional catalysts [6] because they are often easy to prepare from available and cheap precursors and can be separated from the reaction mixture much easier than homogeneous catalysts. Magnetic nanoparticles (MNPs) have also been used as a robust catalyst [32, 33] with a very important feature of straightforward separation using an external magnet bar [34]. This method of separation further

reduces the use of equipment for filtration (*e.g.* centrifuge, membrane filtration) and produces less waste than conventional filtration or centrifugation [35]. MNPs are often easy to prepare, have low toxicity, and are cost-effective. Functionalization of the surface of NPs opens up the possibility of fine-tuning their catalytic properties [36]. However, MNPs have some drawbacks such as tendency of aggregation and alteration of magnetic properties [37]. These problems are usually overcome by surface functionalization and coating of NPs [38].

A number of extensive reviews on MCRs have already been published over the last two decades [1, 2, 12, 39, 40]. Some reviews are focused on gold and silver NP-catalyzed MCRs [41, 42]. A more general overview of the catalysis of organic reactions by NPs has been published in 2013 [43]. This review is focused on the MCRs with cyanide and isocyanate reactants. The reverse C-N bond polarization makes this type of reactants especially versatile building blocks for the construction of nitrogen-containing heterocyclic and linear compounds. The abundance of polar intermediates opens up an opportunity for fine-tuning the NP's surface to optimize its catalytic properties.

2. Synthesis of nanoparticles

A broad classification of the approaches to the NP synthesis encompasses two main classes, *i.e.*, top-down and bottom-up synthesis process summarized

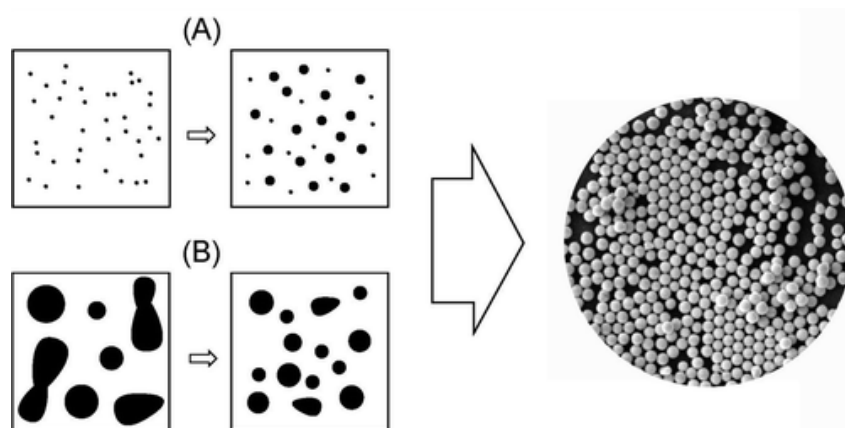
in Scheme 2 [44]. Different approaches to the same type of NPs can produce significantly different materials, because properties and morphology of NPs may be heavily affected by many reaction conditions such as solvent, reaction time, and even the spinning rate of a magnetic stir bar.

2.1. Top-down synthesis

This method follows destructive process of grinding/milling, physical vapor deposition and other decomposition techniques [45]. In this process a macroscopic material is broken into small pieces and thereafter is converted into nanosized particles. The size of NPs depends on the duration of the applied physical action. A group of researchers synthesized ~20-50 nm sized iron oxide NPs by top-down process using oleic acid as solvent [46]. Laser irradiation was used by another group of authors for the preparation of cobalt oxide NPs with an average size of 5.8 ± 1.1 nm [47]. However, the top-down processes are more likely to produce larger amounts of toxic by-products and, therefore, are of more environmental safety concern [48].

2.2. Bottom-up synthesis

In the bottom-up synthetic approach, the NPs are synthesized onto the substrate by assembling each small component (including molecular precursors) into crystals or nanostructures. As the bottom-up synthesis process proceeds through an assembling process, this process is called the building block



Scheme 2. Synthesis of nanoparticles **A)** Bottom-up process, wherein the molecular precursor is disintegrated and grown into monodispersed colloid by stacking **B)** Top-down process wherein large precursors are broken into NPs (Reprinted with permission from Wang, Y. and Xia, Y. 2004, *Nano Letters*, 4(10), 2047-2050. Copyright (2004) American Chemical Society).

process, where a homogeneous solution or gas is used as a precursor. Takezawa and Imai synthesized titanate nano-sheets at 10 nm thickness using the bottom-up synthesis process [49]. The authors synthesized a titanate by stacking TiO_6 monolayers and ammonium ions in a mixture of agar which contains TiF_4 . The biogenic version of bottom-up synthesis of NPs has attracted the interest of researchers owing to the cost effective, green and less toxic nature of the method. Typically, plant extracts, bacteria, yeast, fungi etc. are used as biological agents for the synthesis of NPs. For instance, polyshaped gold NPs (25–30 nm) were synthesized with a high yield by Raghunandan and coauthors by means of a bottom-up process using microwave-exposed *Psidium guajava* leaf extract [48].

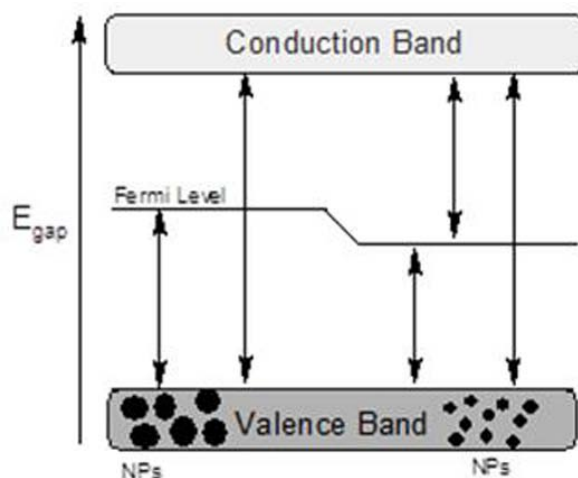
3. Functionalization of nanoparticles

NPs are usually prone to agglomeration driven by the reduction of the surface energy. This is very undesirable for the catalysis applications due to the reduction of the surface area and dispersibility. Besides the control of agglomeration, surface functionalization of NPs is a convenient way to introduce catalytic sites to the surface [33]. For example, surface functionalization of NPs with small molecules or polymeric ligands may create catalytic sites on the NPs' surface (e.g. $-\text{COO}^-$, $-\text{NH}_3^+$, $-\text{CHO}$ etc.) which modifies its binding with the substrate [50]. Therefore, functionalization may enhance both the reaction rate and selectivity. In certain cases, highly active NPs, including MNPs, can be easily oxidized by air and lose their catalytic and magnetic properties [33]. The surface functionalization of magnetic NPs helps to alleviate the alteration of magnetic properties and agglomeration [38]. A plethora of precursors including small molecules (e.g. amino acid, fatty acid, oleic acid, citric acid, cyclodextrin, alkyl phenol, polyol, lycine, alkyl phosphonate, NH_3 etc.), dendrimers, polymers, inorganic materials and biomolecules have been used for the fabrication of NPs' surface.

4. Morphology-dependent catalytic activity of NPs

The NP size normally has a significant effect on its catalytic activity. Smaller particles provide the overall higher surface area improving the contact between the catalyst and its substrates. Bajpai and co-workers studied the catalytic effect of monoclinic- ZrO_2 NPs

of different size and morphology (bulk 2 μm , surface area 6.95 m^2/g), mixed phase NPs (20 nm, surface area 44.70 m^2/g) and single-phase monoclinic NPs (> 10 nm, surface area 69.22 m^2/g) on the synthesis of spirooxindole derivatives [51]. The highest yield was achieved with monoclinic ZrO_2 NPs. The effect of NPs' size on catalytic activity has been also investigated by Kidwai and coauthors for the synthesis of propargylamine derivatives [52]. The maximum reaction rate was observed for about 20 nm NPs, while decreasing size of NPs led to low yields. This counterintuitive result was rationalized by the fact that, the Fermi level shifts downward and thus increases the energy necessary to promote an electron to the conduction band followed by the electron transfer to the adsorbed substrate (Scheme 3). Therefore, the NPs required higher energy for transferring electrons to the adsorbed substrate or ions, which decreased the reaction rate. In contrast, the average particle size above of 20 nm also declines the reaction rate. This happened because the NPs with larger diameter have a lower surface area for adsorption with negligible change of Fermi level. Banerjee and Sereda have reported that 150–200 nm SiO_2 NPs afford a 10% lower yield of pyridine derivatives than 50 nm NPs [53]. The shape of NPs is not less important for the catalytic activity than their size. Thus, the nanorod-shaped Co_3O_4 NPs induced CO oxidation at very low temperature (-77°C) more efficiently than differently shaped Co_3O_4 NPs [54]. We believe it to be due to the presence of active sites specific for the nanorod



Scheme 3. Band gap effect due to the size of nanoparticles.

shape. The catalytic activity of oxidation reduction reaction increased by 51 folds by using the (111) phase of Pt-Ni bimetallic octahedral nanoparticles [55], which provides another example of the morphology-dependent activity of nanocatalysts. Hexagonal pore containing indium-based metal-organic framework (MOF) exhibits outstanding catalytic activity of α -aminonitriles synthesis where metal sites expose Lewis acid centers [56].

5. Influence of reaction medium

The solvent has a profound influence on a reaction's course mostly by its polarity, solvation ability and dissolving power. Thus polar solvents tend to speed up reactions with a more polar transition states (Scheme 4) by lowering the transition state's energy [57, 58]. Chacko and Shivashankar studied the synthesis of α -aminoacyl amide derivatives by using Co_3O_4 nanoparticles [59]. Among a wide range of solvents such as dichloromethane, chloroform, acetonitrile, tetrahydrofuran, benzene, toluene, xylene and water, only methanol afforded a good yield of the product [58]. This is not surprising for the most polar methanol, able to dissolve the reactants and stabilize the polar intermediate of Ugi reaction.

Another example of the excellent yield of 4*H*-pyran derivatives in polar water and ethanol was reported by Zakeri and coauthors [61]. In addition, the dispersibility of NPs in methanol is very high which results in a quasi-homogenous system with a very high surface area of the catalyst [62]. Although the polarity of water and acetonitrile is higher than that of methanol, the lower yields in those solvents may be due to the lower solubility of the reactants. Aprotic solvents (*e.g.* CH_2Cl_2 , CH_3CN , CHCl_3 , dimethylformamide, tetrahydrofuran) favor the Passerini reaction and polar-protic solvents

(*e.g.* methanol) are preferred for Ugi reaction [63]. The Passerini reaction lacking a nucleophilic amine as a reagent, apparently, benefits from the aprotic solvents stimulating nucleophilicity.

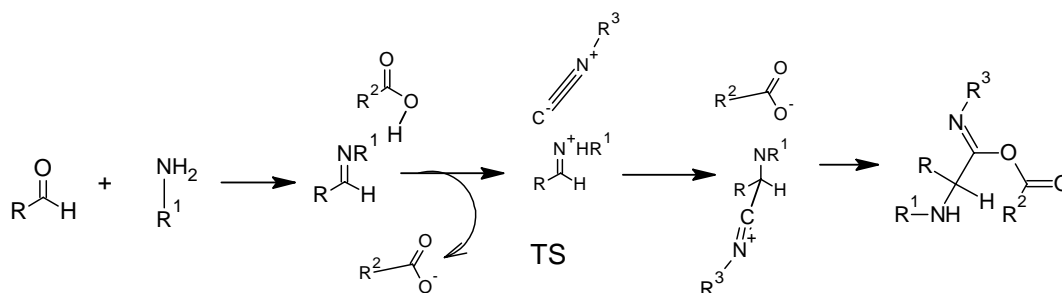
In the past decades, a plethora of compounds have been synthesized under solvent-free conditions, which are more economical and environmentally friendly. As Toda concluded in 1995 "no solvent is perfect solvent" [64]. The field of MCRs was not escaping the trend. In 2017, a group of authors introduced SiO_2 -coated Fe_3O_4 MNPs as a solvent-free catalyst (catalyst?), and observed higher yields compared to the solvent medium [65], which may be due to the absence of solvation. In the same year, Singha *et al.* reported that highly spherical, crystalline and single phase CuO NPs synthesized from Cu-based MOF demonstrate excellent catalytic effect for the synthesis of α -aminonitriles in a solvent-free medium [66].

6. MCR catalyzed by functionalized nanoparticles

6.1. MCRs catalyzed by metal-oxide NPs

Metal-containing NPs are potential candidates as catalyst by virtue of their high activity, tunability and recyclability [67-69]. Nano-catalysts often provided excellent yields due to their unique physical and chemical properties. Thus, metal oxides show higher surface area to volume ratios which contributes to catalytic activity [70]. The effects of metal oxide NPs on some MCR yields are summarized in Table 1.

This type of catalysts has been proven to be especially useful for accessing α -aminonitrile-precursors of synthesis of amino acids [80], amides, diamines [81] imidazoles and thiadiazoles [82]



Scheme 4. Charged species of transition state [60].

Table 1. MCRs catalyzed by metal oxides nanoparticles.

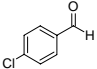
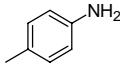
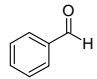
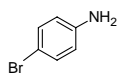
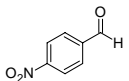
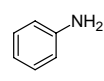
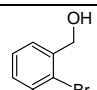
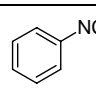
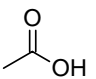
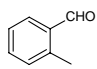
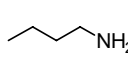
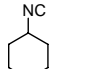
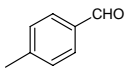
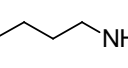
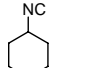
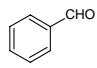
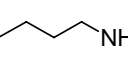
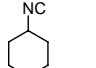
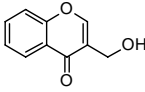
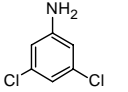
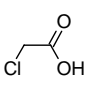
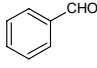
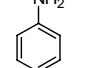

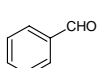
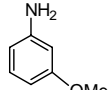

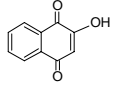
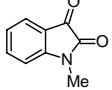
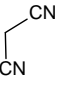
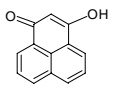
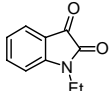
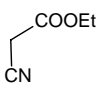
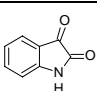
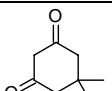
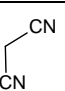
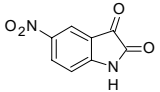
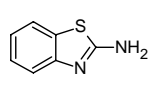
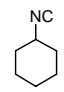
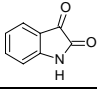
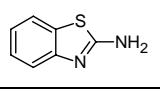
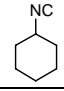
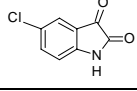
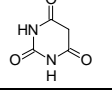
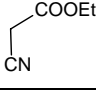
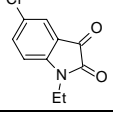
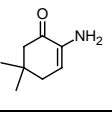
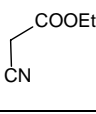
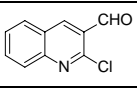
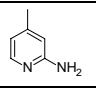

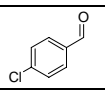
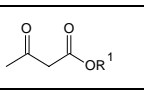
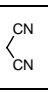
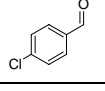
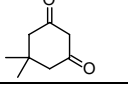
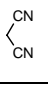
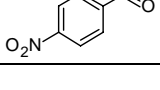
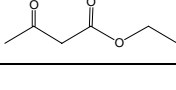
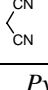
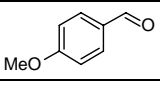
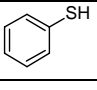
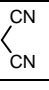
A1	A2	A3	Catalyst	Time	% Yield	Catalytic recycle no.	Ref.
<i>α-aminonitrile</i>							
		TMSCN	Acidic CuFe ₂ O ₄	73 min	92	4	[71]
		TMSCN	Acidic CuFe ₂ O ₄	75 min	94.5		
		TMSCN	Acidic CuFe ₂ O ₄	55 min	98		
<i>α-acyloxy amide</i>							
			CuCl ₂ - TEMPO	24 h	80	-	[72]
<i>α-aminoacyl amide</i>							
$R^1-CHO + R^2-NH_2 + R^3-COOH + R^4-NC \longrightarrow R^1-C(=O)-N(R^2)-CH(R^3)-C(=O)-R^4$							
			Fe ₃ O ₄	4 h	95*		[60]
			Fe ₃ O ₄	4 h	94	3	
			-	24 h	54		
			Co ₃ O ₄	2 h	84**	-	[59]
			ZnO	5 h	90	-	[73]
			ZnO	7 h	88	-	
<i>Spirooxindole derivatives</i>							
			CuFe ₂ O ₄	30 min	97	4	[74]
			-	30 min	23		
			SBA-Pr-NH ₂	5 min	91	4	[75]

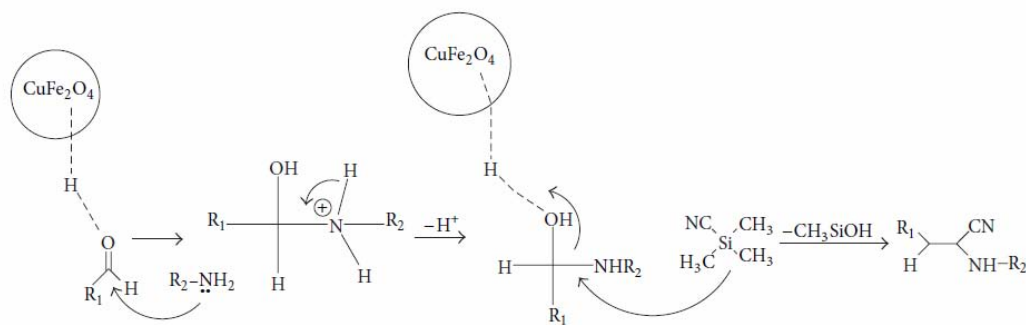
Table 1 continued..

			TiO ₂	2 h	96	5	[76]
			-	>10 h	Trace		
			monoclinic-ZrO ₂	35 min	97***	10	[51]
			monoclinic-ZrO ₂	35 min	96		
<i>Imidazole derivatives</i>							
			γ-Fe ₂ O ₃	2 h	96	5	[77]
<i>4H-pyran derivatives</i>							
$R^1CHO + \begin{matrix} \diagup \\ CN \\ \diagdown \end{matrix} + \begin{matrix} O \\ \\ R^2-CH_2-CH_2-C(OR^3) \end{matrix} \longrightarrow \begin{matrix} OR^1 & R^2 & CN \\ & & \\ & C & C \\ & / & \backslash \\ & O & NH_2 \end{matrix}$							
			SiO ₂	2 h	88 [†]	8	[78]
			SiO ₂	20 min	98		
			ZnO	2.5 h	98	5	[79]
<i>Pyridine derivatives</i>							
			SiO ₂	2.5 h	85	-	[53]

- Highest yield is tabulated; TMSCN = trimethylsilyl cyanide; *R³ = -CH₃; **Isocyanide source is t-butyl isocyanide; ***Ball milling yield; [†] at 80 °C.

and other bioactive compounds including anti-tumour saframycin A [83]. Acidic CuFe₂O₄ nanoparticles were used by Ghaib and coauthors as a “green” catalyst to synthesize an α-aminonitrile in water at room temperature [71]. The authors reported 98% yield in 55 min. In control experiments, the reaction did not take place without the catalysts. Relatively higher yields were observed for electron-deficient aromatic aldehydes, which might be due to the intermediate acting as a better hydrogen bond acceptor with the acidic copper ferrite (Scheme 5). α-Acyloxy amides, such as azinomycin [84], analogues of serine [85], cysteine [86], have a

variety of pharmacological activities [87]. In a conventional Passerini reaction, an aldehyde or ketone, carboxylic acid and isocyanides are condensed into an α-acyloxy amide. The aldehyde is condensed as a main reactant in Passerini reaction, which limits its versatility [88]. However, in a modified version of the reaction, an aldehyde can be replaced with an alcohol, which widens the versatility and scope of the process [89-91]. Other modifications of Passerini reaction employ a trimethylsilyl azide [92], thioacids [93], silanol [94], or ketene instead of the carboxylic acid reactant [95]. Briche and coauthors have reported a protocol by using a TEMPO (2,2,6,6-tetra-methyl-piperidin-1-oxyl)

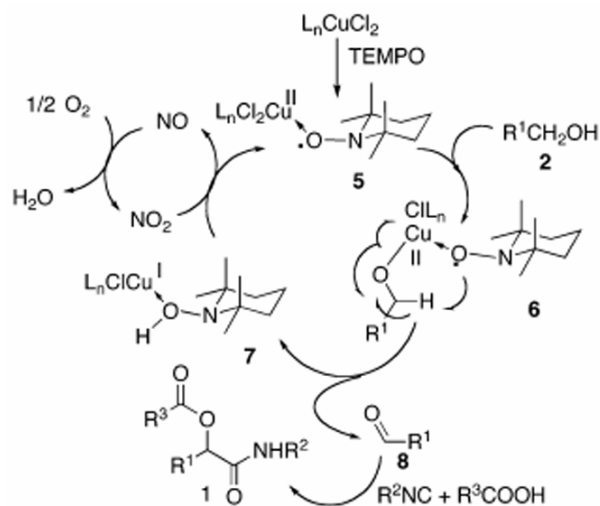


Scheme 5. α -Aminonitrile synthesis catalyzed by acidic CuFe_2O_4 (Reproduced from Gharib, A., Noroozi Pesyani, N., Vojdani Fard, L. and Roshani, M. 2014, *Organic Chemistry International*, 2014, 1-6).

nanoparticle catalyst for the synthesis of α -acyloxy amide derivatives with moderate to good yield under mild conditions [72]. TEMPO is an aminoxide that catalyzes oxidation of primary alcohols to aldehydes with oxygen as the oxidizing agent. The CuCl_2 -TEMPO- NaNO_2 NPs (2.5 equiv %) afforded much better yield (65%) compared to FeCl_3 -TEMPO- NaNO_2 (30%). The authors used oxygen as an oxidant and CuCl_2 -TEMPO hybrid nanoparticles as a catalyst [72, 96]. In the catalytic cycle, NaNO_2 provides NO and acts as co-catalyst for O_2 activation (Scheme 6). The metal chlorides coordinate with both the alcohol and the N-oxide species, bringing them together.

Synthesis of α -aminoacyl amides conventionally used as pharmaceutical and agricultural agents, *via* the four-component Ugi reaction is very straightforward. They exhibit excellent anticancer [97, 98], anaesthetics [99], antibiotics [100], and antibacterial [101] activity. Ghavami and coauthors applied functionalized Fe_3O_4 NPs to catalyze Ugi reaction [60]. They also reported that, the copper (II) acetylacetonate-functionalized silica NPs provide an excellent yield (87-96 %) for aromatic aldehydes unless heteroaromatic (*e.g.* pyridine, pyrrole) aromatic aldehyde. Without the catalyst, the product was formed only at the 10% yield. The maximum yields of α -aminoacyl amides were achieved at the 0.85 mol % of the catalyst content. The authors speculated that the nano-catalysts coordinate with the carbonyl group of the aldehyde, increasing its electrophilicity at the step of the imine formation (Scheme 7).

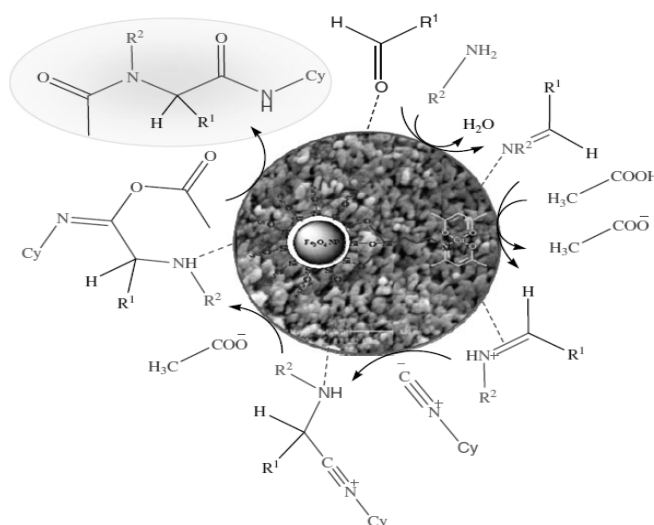
While the conventional Ugi reaction involves four components, Kumar and co-researchers developed



Scheme 6. CuCl_2 -TEMPO- NaNO_2 NP-catalyzed mechanism for the synthesis of α -acyloxy amide derivatives (Reprinted with permission from Brioché, J., Masson, G. and Zhu, J. 2010, *Organic Letters*, 12(7), 1432-143. Copyright (2010) American Chemical Society).

a three-component Ugi type reaction of aldehyde, amine and isocyanide to prepare α -arylamino phenylacetimidamide at a satisfactory yield, using ZnO NPs as catalysts [73]. The authors also reported that TiO_2 NP failed to catalyze this reaction.

The spirooxindole moiety is present in a range of pharmacologically active compounds such as alkaloids [102]. The derivatives of spirooxindole have potential application as antimicrobial [103], antitumor [104] and other pharmaceutical agents [105]. Bazgir and coauthors synthesized antibacterial and antifungal spirooxindoles at high to excellent yields under mild conditions in water with copper



Scheme 7. The role of nanoparticles in Ugi reaction (Reproduced from Ghavami, M., Koochi, M. and Kassaee, M. Z. 2013, *Journal of Chemical Sciences*, 125(6), 1347-1357).

ferrite (CuFe_2O_4) NP as the catalyst [74]. The authors pointed out that the Nps retained high activity even after being recycled for five times. Without the catalyst, the product was obtained at the low yield of 23% only.

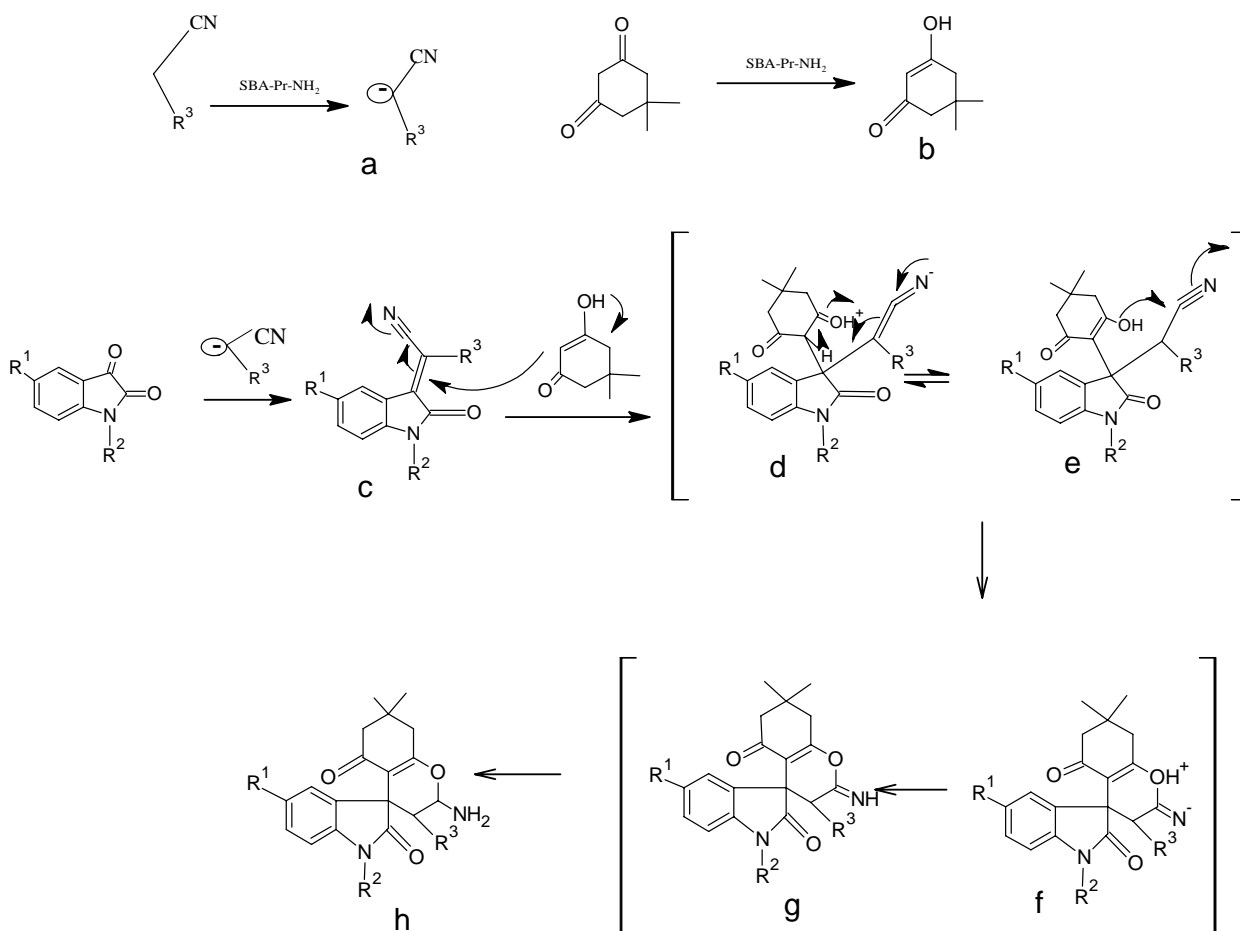
Santa Barbara Amorphous (SBA)-type mesoporous silica NP has recently drawn the attention of researchers. The SBA-Pr- NH_2 NPs were used by a group of researchers for the synthesis of spirooxindole derivatives in aqueous medium at good to excellent yields [75]. The catalyst was separated from the reaction mixture by filtration and reused up to four times with a 20% decrease in catalytic activity. The authors suggested a reaction mechanism (Scheme 8) where amino-functionalized SBA-15 nanoparticles play a significant role in the catalytic cycle. The reaction might be initiated through the deprotonation of cyanoacetic ester or malononitrile **a** by the SBA-Pr- NH_2 NP. Similar to the Knoevenagel reaction, the isatylidene-malononitrile intermediate **c** is formed. Next, the adducts **d** and **e** are produced by the addition of enole **b** to **c**. Finally, cyclization of hydroxyl group with cyano moiety affords the spirooxindole derivative **h**.

An efficient protocol for the synthesis of spirooxindole derivatives catalyzed by TiO_2 NPs has been reported [76]. The authors achieved excellent yields of spirooxindole derivatives in aqueous ethanol (3:2) at 90 °C from 2-aminobenzothiazole, cyclohexyl isocyanide and isatines. Only a trace

amount of the product was detected after 10 h without the catalyst. They also observed a good yield (70% in 5 h) with ZnS NPs as a catalyst.

Bajpai and co-workers introduced a solvent-free green technique for the synthesis of spirooxindole derivatives catalyzed by monoclinic- ZrO_2 NPs [51]. The reaction was performed by grinding isatin derivatives, 1,3-dicarbonyl compounds and ethyl cyanoacetate in a ball mill producing spirooxindole derivatives with excellent yield. The highest yield (97%) was achieved with 20 mol % of catalyst. The NPs were separated from the reaction mixture by centrifugation and reused up to 10 times without substantial decrease of catalytic activity. The rotation frequency as well as the quantity of milling balls significantly affected the reaction. The maximum yield was observed at 800 rpm with 16 balls (made of Al_2O_3 , 10 mm diameter).

The imidazole polycyclic compounds are known for various pharmacological activities [106]. They have been proven to be effective antibacterial [107], antimicrobial [108], anticancer [109], antitumor [110], anti-inflammatory [111], and antialzheimer [112] agents as well as gastric acid secretion inhibitors [113]. Modified iron oxide NPs have been explored for the synthesis of imidazole derivatives under solvent-free condition [77]. The authors used sulfamic acid-functionalized and hydroxyapatite-encapsulated $\gamma\text{-Fe}_2\text{O}_3$ nanoparticles (10 mol %) which afforded good to excellent yields.



Scheme 8. Mechanism of the catalytic synthesis of spirooxindole.

Sereda and his group reported the synthesis of *4H*-pyran derivatives using highly stable SiO₂ NPs under elevated temperature [78]. Compounds with the *4H*-pyran moieties often exhibit a plethora of significant biological and pharmacological activities including spasmolytics, diuretic, anti-coagulant, anti-cancer and anti-anaphylactic properties. They are candidates for the treatment of neurodegenerative disorders, amyotrophic lateral sclerosis, Parkinson's disease, Alzheimer's disease and Huntington's disease [114, 115]. The authors produced the target compounds from a series of aldehyde derivatives, malononitrile, and 5,5-dimethyl-1,3-cyclohexanedione, at excellent yields (86-98%). Interestingly, the aryl aldehyde derivatives give better yields in a shorter time compared with their alkyl counterparts. The presence of an electron-donating group in the *para* position of an aromatic aldehyde further facilitated the reaction. However,

replacement of 5,5-dimethyl-1,3-cyclohexanedione with ethyl acetoacetate led to the synthesis of *4H*-pyran derivatives at very good yields within 2 h at 80 °C. A similar process with an increased relative amount of malononitrile and a monoketone instead of the dicarbonyl reactant at 70 °C afforded poly-substituted anilines at moderate yields (52-65%). The Sereda's group extended the use of SiO₂ NP to the synthesis of a series of pyridine derivatives at moderate to good yield (60-85%) [53]. As opposed to DMF and acetone, the good yields have been achieved only if ethanol was employed as the solvent.

Bhattacharyya *et al.* also synthesized *4H*-pyran derivatives at good to excellent yields using ZnO NPs as a catalyst [79]. The highest yield was observed in ethanol and water-ethanol mixture (1:1) as solvents. The electron withdrawing groups in *para*- and *meta*- position of aromatic aldehydes afford better yield compared to electron donating groups.

Although Sereda and coauthors [78] found higher catalytic activity of SiO₂ NPs for 4*H*-pyran synthesis, Bhattacharyya *et al.* did not observe the efficient-enough catalytic activity of bulk SiO₂ for a similar reaction. They observed that CaO and MgO do not show any catalytic activity, while, Al₂O₃ NPs and bulk ZnO afford moderate yields of the product (32-42% and 68%, respectively). Recently, a metal-free catalyst (graphene oxide-phosphoric acid) was reported to catalyze a four-component synthesis of 4*H*-pyran derivatives with excellent yield (90%) within 15 min [61]. The catalytic activity is attributed to the presence of acidic and basic sites on the catalyst's surface. Remarkably, the reaction proceeded in a green solvent (H₂O) and the catalyst was reused for 6 times with high recovery (98%) and negligible loss

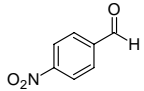
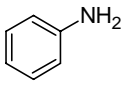
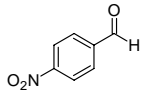
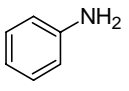
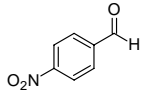
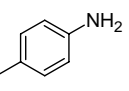
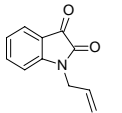
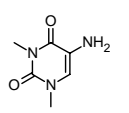
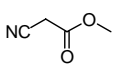
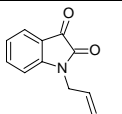
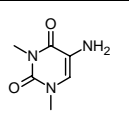
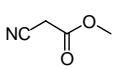
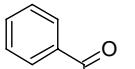
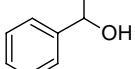
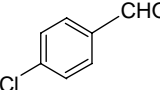
of activity (1%). This functionalized graphene oxide catalyst is most active in protic solvents (*e.g.* H₂O and C₂H₅OH) compared to polar aprotic solvents (*e.g.* DMF, DCM, THF, CHCl₃ and CH₃CN).

6.2. Multicomponent reactions catalyzed by magnetic nanoparticles

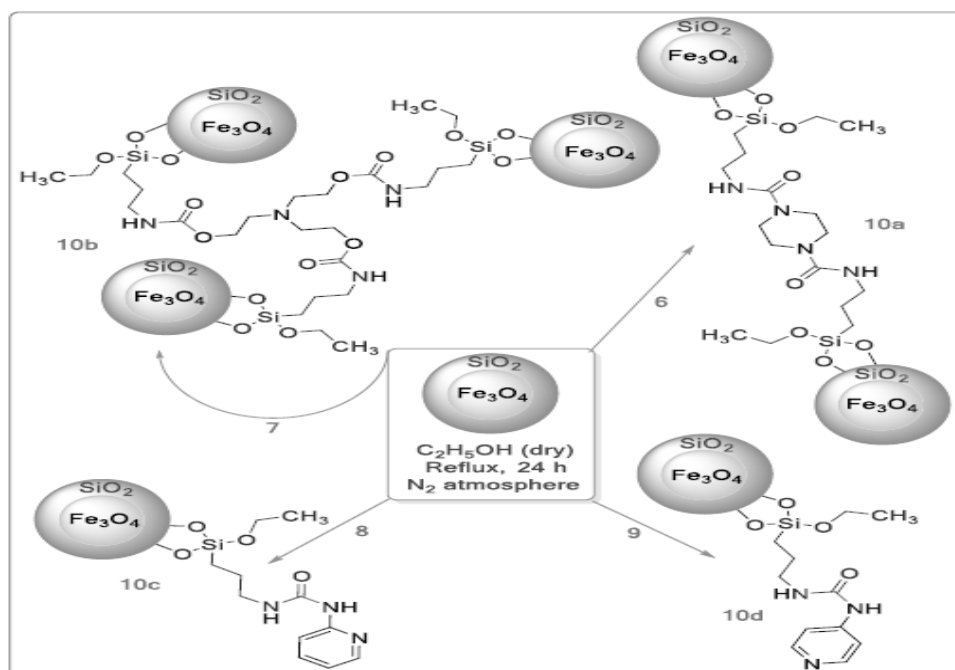
While MNPs are often readily oxidized in air and lose their magnetism as well as dispersibility in many solvents, this type of problems can be remediated by post-synthetic surface modification. In addition, the catalytic sites can be engineered on the surface [27]. The catalytic effects of MNPs on some MCRs are summarized in Table 2.

A group of authors recently applied four different novel Fe₃O₄-based MNPs (Scheme 9) for the synthesis of α -aminonitrile derivatives at 50 °C under

Table 2. MCRs catalyzed by magnetic nanoparticles.

A1	A2	A3	Catalyst	Time	% Yield	Recycled catalyst	Ref.
<i>α-aminonitrile derivatives</i>							
		TMSCN	-	1 h	-	-	[65]
		TMSCN	Fe ₃ O ₄ (10a)	15 min	93	7	
		TMSCN		10 min	95		
<i>Spirooxindole derivatives</i>							
			Acidic Fe ₃ O ₄	12 h	96*	5	[116]
			-	24 h	-		
<i>Imidazole derivatives</i>							
 		NH ₄ OAc	Fe ₃ O ₄	50 min	95	6	[117]

- Highest yield reported in table; *Yield recorded at 80 °C.



Scheme 9. SiO₂-coated Fe₃O₄ magnetic nanoparticles (Reproduced from Bagheri, S., Zolfigol, M. A., Schirhagl, R., Hasani, M., Stuart, M. C. and Nagl, A. 2017, *Applied Organometallic Chemistry*, 31(12), e3883).

solvent-free condition at 77-94% yield [65]. Without the catalyst, the reaction yield was 15%. The yield under the solvent-free conditions was much higher than in any of the tested solvents: water, methanol, acetonitrile, dichloromethane, *n*-hexane, ethylacetate and toluene. This might be due to the solvation effect and ion pairing effect in solution, which deactivates the key intermediates.

This reaction proceeded faster with aromatic aldehydes containing electron withdrawing substituents than with those containing electron donating groups. The aromatic aldehydes were more reactive than their aliphatic counterparts. In contrast, the aliphatic amines showed faster reaction rates, shorter reaction time, and led to higher yields than aromatic amines. This may be attributed to the deactivation of the nucleophilic lone electron pair in aromatic amines by resonance. Among the four catalysts, **10a** (Scheme 9) was found to be most active which may be due to the heterocyclic backbone in its core structure, enhancing its hydrogen bond acceptor capabilities.

Karimi and coworkers introduced magnetic core shell NPs coated by TEMPO for domino aerobic oxidative Passerini reaction in halogen free

environment and reported good to excellent yields of α -acyloxy amide derivatives [88]. The authors also used *t*-butyl nitrite (TBN) which enhanced the activity of TEMPO and reduced its required amount from 1.5 mol% to 1.0 mol%. Out of the explored series of isocyanides, benzyl isocyanide resulted in the best yields (84-92%). Primary alcohols led to better yields than secondary ones. There was just a negligible change in the catalyst's activity after it was reused 14 times.

Another (tungstic acid) derivative of Fe₃O₄ NP reported to catalyze formation of spirooxindoles at moderate to good yields [116]. No product was detected without the catalyst. Silica coated MNPs also did not catalyze the reaction to a significant extent (10% after 24 hours). However, they afforded excellent yield (93%) in 8 hours upon refluxing in water. It was found that tungstic acid itself provided just a moderate yield (60%) of the product. The authors reused the MNPs up to six times without noticeable loss of catalytic activity.

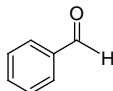
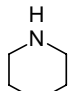
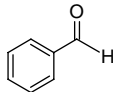
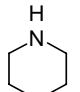
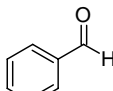
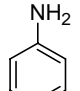
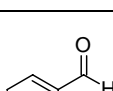
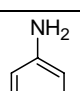
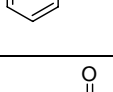
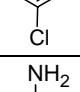
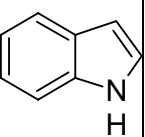
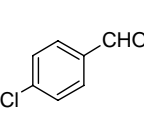
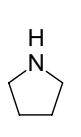
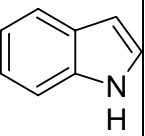
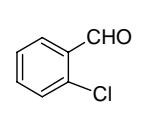
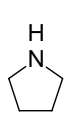
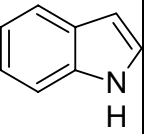
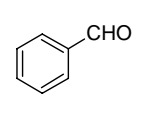
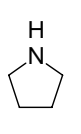
A series of imidazole derivative was synthesized using *o*-phthalaldehyde, trimethylsilyl cyanide and 2-aminopyridines with a catalytic amount of amine functionalized iron oxide (Fe₃O₄) MNPs

under ultrasonic (frequency 40 kHz) irradiation [117]. After 10 min, the reaction afforded 85-95 % yield in ethanol. In this experiment, a range of solvents like H₂O, MeOH, MeCN, CH₂Cl₂, toluene and EtOH as well as solvent free conditions were explored. The best yield was achieved in EtOH as the solvent. The nanoparticles were separated with an external magnetic bar and reused five times without significant loss of catalytic activity.

6.3. MCRs catalyzed by nano-composites

In recent years, nano-composites have been attracted significant attention because of the capability of combining different phases with desired properties, such as magnetic phase and a very high surface area mesoporous phase [118-120]. The yields of MCRs catalyzed by magnetic composite materials are tabulated in Table 3.

Table 3. MCRs catalyzed by nano-composites.

A1	A2	A3	Catalyst	Time	% Yield	Recycled catalyst	Ref.
<i>α-aminonitrile derivatives</i>							
		TMSCN	-	2 h	18**	-	[121]
		TMSCN	magnetic (Fe ₃ O ₄ /g-C ₃ N ₄)	2 h	97**	5	
		TMSCN	MIL-101(Fe)@Fe ₃ O ₄	35 min	98	5	[122]
		TMSCN	MIL-101(Fe)@Fe ₃ O ₄	30 min	97	5	
		TMSCN	MIL-101(Fe)@Fe ₃ O ₄	90 min	95	5	
<i>Indole derivatives</i>							
			*RGO/ZnO	20 min	90	6	[123]
			*RGO/ZnO	30 min	85	6	
			-	10 h	-	-	

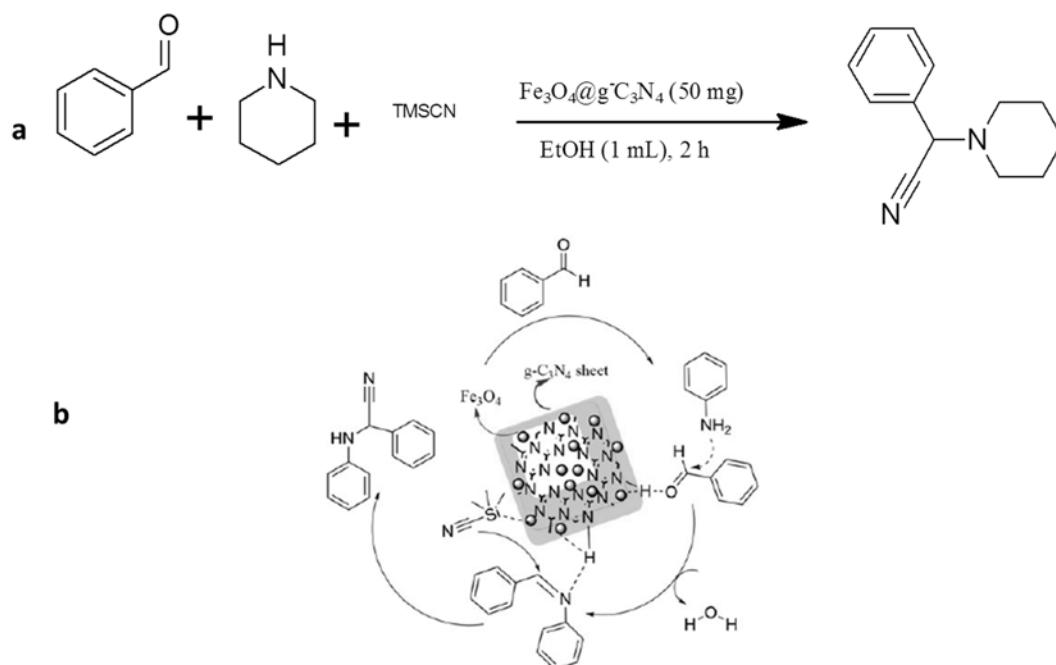
- Highest yield reported in this table; *Reduced Graphene Oxide; ** Yield at 75 °C; TMSCN = trimethylsilyl cyanide.

Azizi and Farhadi studied the synthesis of α -aminonitrile (Scheme 10a) catalyzed by magnetic graphitic carbon nitride ($\text{Fe}_3\text{O}_4/\text{g-C}_3\text{N}_4$) composite [121]. The researchers observed good to excellent yields (40-97%) of α -aminonitrile, while without the catalyst, the yield was only 18%. The ethanol solvent afforded an excellent yield of 97% compared to 78% in DMF and only 40% for toluene. The authors proposed a mechanism for the preparation of α -aminonitrile (Scheme 10b) where benzaldehyde forms hydrogen bond with functionalized $\text{Fe}_3\text{O}_4/\text{g-C}_3\text{N}_4$ and is activated to form an imine by reacting with aniline. After that, the activated trimethylsilylcyanide reacts with activated imine and forms an α -aminonitrile. The authors' explanation of the mechanism involves hydrogen bonding interactions, hydrophobic interactions, π - π interactions and Van der Waals interactions.

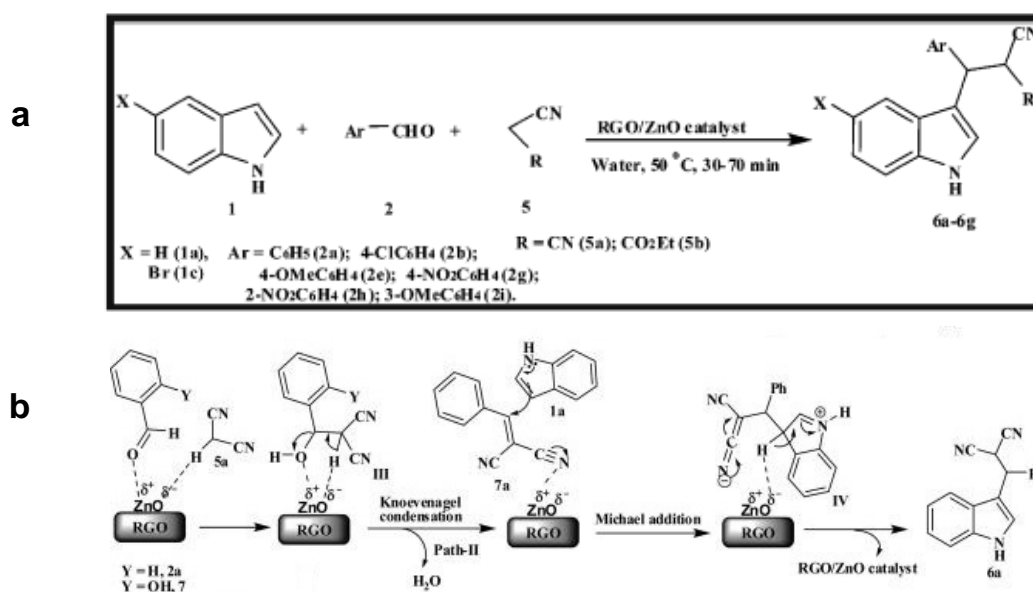
Highly porous MIL-101(Fe) and ferric oxide nano-composites have also been used to catalyze the synthesis of α -aminonitrile in ethanol at room temperature using trimethylsilylcyanide instead of traditional metal cyanides (e.g. KCN, NaCN) [122]. The MIL-101(Fe) NP led to the formation of an α -aminonitrile at 85% yield, while Fe_3O_4

NPs afforded 65% yield. However, the catalytic activity of nanocomposites prepared from the combination of Fe_3O_4 and MIL-101(Fe) boosted the yield to 98% at room temperature. The catalyst was reused up to five times with negligible loss of activity (2%) and recovery loss (3%).

The indole moiety is often responsible for the activity of bioactive natural products, agrochemicals and pharmacologically active molecules and also is usually present in the intermediates for their synthesis [124, 125]. A nano-composite of reduced graphene oxide (RGO) and zinc oxide has been introduced for the synthesis of indole derivatives in water at 50 °C (Scheme 11a) at excellent yields [123]. It is noteworthy to mention that, electron donating substituents (e.g. OMe, OH) at *meta* and *para* positions of the aldehyde showed slightly lower reactivity compared to those with electron withdrawing substituents (e.g. NO_2 , Cl) at *ortho* and *para* positions. According to the proposed mechanism, (Scheme 11b) an aldehyde first reacts with malononitrile on the basic site (oxide-ions) of ZnO which is followed by dehydration. The nucleophilic attack of indole on the conjugated methine then occurs at the Zn^+ sites of ZnO.



Scheme 10. a) Synthesis of α -aminonitrile b) Mechanism of the synthesis of an α -aminonitrile (Reproduced from Azizi, N. and Farhadi, E. 2018, Applied Organometallic Chemistry, 32(3), e4188).



Scheme 11. **a**) RGO-catalyzed synthesis of indole derivatives **b**) Possible mechanism for the synthesis of indole derivatives (Reprinted with permission from Rajesh, U. C., Wang, J., Prescott, S., Tsuzuki, T. and Rawat, D. S. 2014, ACS Sustainable Chemistry & Engineering, 3(1), 9-18. Copyright (2015) American Chemical Society).

6.4. MCRs catalyzed by nanoscale metal organic frameworks

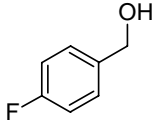
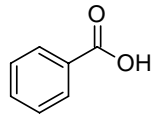
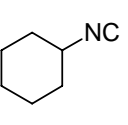
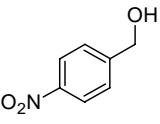
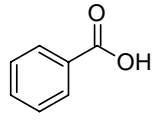
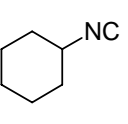
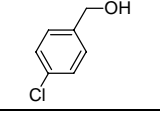
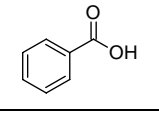
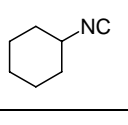
Metal-organic frameworks (MOFs) are two-dimensional or three-dimensional coordinated polymers that contain metal ion bridged with organic ligands [126]. Those structural elements often comprise a porous framework with unique features and functional properties [127]. MOFs can be crystalline, and their surface areas can reach ultrahigh values up to 10000 m²/g, which is unique, and have versatile uses [128]. The modification of MOFs by changing organic linker molecules and metal ions might afford uniform cavities, and tailorable physicochemical properties [129, 130]. Nano-sized MOFs exhibit cavities and/or open channels [131] both in the metal ions and organic linker sub-frameworks [132, 133]. This allows for the higher surface area, which enhances their catalytic activity, and therefore, increases the yield of the product. The Van der Waals attraction and solvophobic effects may contribute to the catalytic activity of MOFs [134]. By changing the organic linker molecules the catalytic activity can be tuned to favour a specific reaction. Table 4 summarizes the examples of using MOFs as catalysts for MCRs.

A zirconium-based MOF known as UiO-66, which is thermally, mechanically and chemically stable

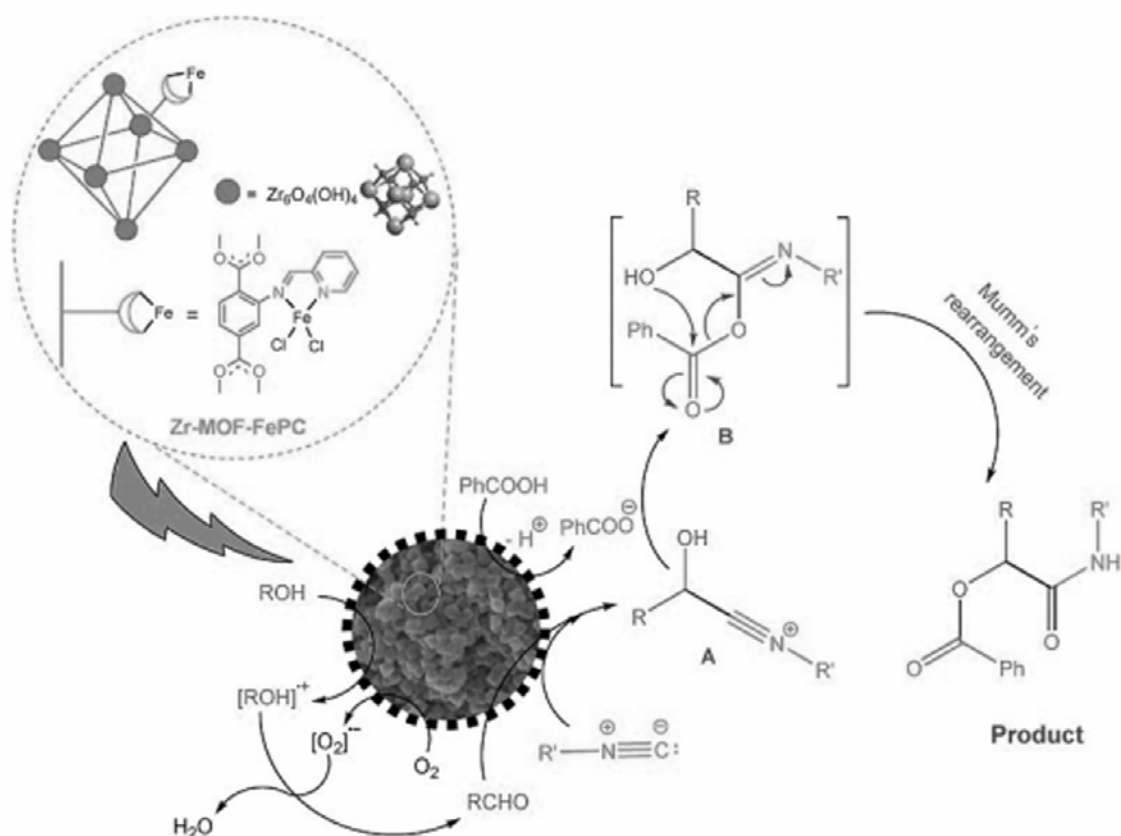
and has high coordination number owing to its Zr(IV)-O bond, has been used to study the synthesis of α -acyloxy amide derivatives by Azarifar and coauthors [134]. The reaction starts with the UV-initiated photo oxidation. The authors proposed that the reaction sequence was initiated by the oxidation of alcohol to the corresponding aldehyde under UV light and air over the Zr-based MOF catalyst (Scheme 12). The resulting aldehyde reacts with the isocyanide and forms an intermediate imine. Next, the imine reacts with the carboxylate anion and affords the α -carboxyl amides derivatives. The effect of different substituents on the reactivity of the alcohol reactant was negligible. No product was formed without the catalyst and UV irradiation.

A zirconium-based porous multifunctional MOF also efficiently catalyzed the photo-oxidative Passerini reaction [134]. The authors observed 81% yield of α -acyloxy amide by reacting 4-chlorobenzyl alcohol, benzoic acid and cyclohexyl isocyanide in the presence of 40 mg of MOF under UV radiation at room temperature. No product was detected in the absence of the catalyst or UV radiation. In the absence of UV irradiation, the catalyst afforded a much lower yield of 59%. They authors observed the best yield in the acetonitrile solvent and explained it by the longer lifetime of the intermediate singlet oxygen.

Table 4. MCRs catalyzed by MOF.

A1	A2	A3	Catalyst	Time	% Yield	Recycled catalyst	Ref.
<i>α-acyloxy amide</i>							
			Zr-MOF-FePC*	26 h	81	-	[134]
			Zr-MOF-FePC*	24 h	77	-	
			Zr-MOF-FePC	28 h	81†	3	[134]

- Highest yields are tabulated; *Fe(III)-pyridinecarboxaldehyde-functionalized zirconium-based metal-organic framework; †under UV irradiation.



Scheme 12. Proposed mechanism for the MOF catalyzed synthesis of α -acyloxy amide derivatives (Reproduced from Azarifar, D., Ghorbani-Vaghei, R., Daliran, S. and Oveisi, A. R. 2017, ChemCatChem, 9(11), 1992-2000).

6.5. Catalysis of MCRs by bionanostructures

Functionalization of nanoparticles with biopolymers (e.g. chitosan, cellulose, proteins etc.) may enhance the catalytic activity and results in “greener” and more sustainable catalysts known as bionanostructures with tunable compositions, phases, internal interfaces, and morphology [135-137]. The catalysts of this type are often nontoxic, biodegradable, biocompatible and ecofriendly [138]. Several examples of MCRs catalyzed by bionanostructures are listed in Table 5.

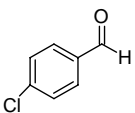
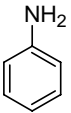
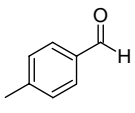
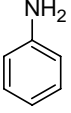
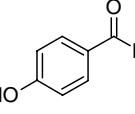
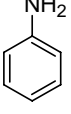
A catalyst made of CuFe_2O_4 MOF-NPs has been applied for the synthesis of α -aminonitrile derivatives by Maleki and coworkers [139]. They synthesized α -amino nitriles from aryl aldehydes, aromatic amines and trimethylsilyl cyanide in ethanol at room temperature at excellent yields (87-95% in 15 min). Slightly better yields were observed for the reactant aldehydes with electron withdrawing substituents

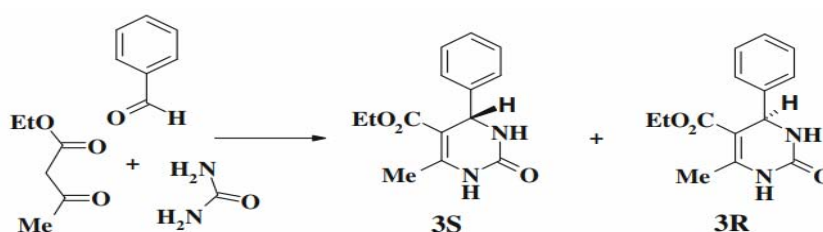
at the *p*-position, when compared with their electron donor-substituted counterparts.

7. Effect of NPs on chiral catalysis

Asymmetric catalysis is an indispensable method for the synthesis of optically active precursors of pharmaceutically important compounds [140-143]. NPs enhance the activity of asymmetric catalysts used for stereoselective synthesis. Thus, carbon encapsulated Ni and Cu NPs increased the stereoselectivity (Scheme 13) of the chiral *L*-proline catalyst [144]. The authors observed 18% more *S*-enantiomer with the heterogeneous catalyst whereas in the case of the homogeneous catalyst the value was very low. The best yields were observed using carbon-encapsulated Ni NP modified with chiral *L*-proline. The maximum yield ratio of *S* and *R* was observed at 59:41% which is comparatively better than carbon-encapsulated Cu NP-modified catalyst (*S*:*R* enantiomers are 51:49%).

Table 5. MCRs catalyzed by bionanostructured materials.

A1	A2	A3	Catalyst	Time	% Yield	Recycled catalyst	Ref.
<i>α-aminonitrile derivatives</i>							
		TMSCN	$\text{CuFe}_2\text{O}_4/\text{chitosan}$	15 min	94	5	[139]
		TMSCN		15 min	91		
		TMSCN		15 min	88		



Scheme 13. Stereoselective synthesis of 3,4 dihydropyrimidine enhanced by Ni and Cu NPs with *L*-proline (Reproduced from Uhm, Y. R., Lee, H. M., Olga, F., Irina, O., Marina, V., Gennady, R., Valery, C. and Rhee, C. K. 2010, *Research on Chemical Intermediates*, 36(6-7), 867-873).

8. Conclusion

The multicomponent reactions are still an ongoing research interest in the field of synthesis of heterocyclic compounds. MCRs allow for higher yields, better atom economy and lower side product generation. Nano-catalysts already established a new window in the research of multicomponent reactions. Nano-catalysts further expand the synthetic value of MCRs by increasing the yields, decreasing reaction time, reusing the catalyst for multiple reaction runs, and allowing “green” processes in aqueous solvents or with no solvent at all. The engineering of hybrid catalysts opens the door for readily separable magnetic nanoparticles and versatile surface functionalized materials.

ACKNOWLEDGEMENTS

Authors are indebted to Dr. Rick Wang for the helpful discussions, and the department of chemistry of the University of South Dakota for financial support.

CONFLICT OF INTEREST STATEMENT

The authors do not have any conflict of interests.

REFERENCES

- Dömling, A. 2006, *Chemical Reviews*, 106(1), 17-89.
- Hulme, C. and Gore, V. 2003, *Current Medicinal Chemistry*, 10(1), 51-80.
- Strecker, A. 1850, *European Journal of Organic Chemistry*, 75(1), 27-45.
- Dolle, R. E. and Nelson, K. H. 1999, *Journal of Combinatorial Chemistry*, 1(4), 235-282.
- Weber, L. 2002, *Current Medicinal Chemistry*, 9(23), 2085-2093.
- Gundala, T. R., Kumar, G. and Reddy, N. G. 2018, *Advanced Synthesis & Catalysis*, 360, 1-13.
- Weber, L. 2000, *Current Opinion in Chemical Biology*, 4(3), 295-302.
- Zhu, J. 2006, John Wiley & Sons.
- Ugi, I. 1997, *Advanced Synthesis & Catalysis*, 339(1), 499-516.
- Passerini, M. 1921, *Gazz. Chim. Ital*, 51, 181-189.
- Ugi, I., Meyr, R. and Fetzer, U. 1959, *Angew. Chem*, 1959. 71, 386.
- van Berkel, S. S., Bögels, B. G., Wijdeven, M. A., Westermann, B. and Rutjes, F. P. 2012, *European Journal of Organic Chemistry*, 2012(19), 3543-3559.
- Dömling, A. and Ugi, I. 2000, *Angewandte Chemie International Edition*, 39(18), 3168-3210.
- Nogata, Y. and Kitano, Y. 2006, Springer, 87-104.
- Hantzsch, A. 1882, *European Journal of Organic Chemistry*, 215(1), 1-82.
- Mori, K. 2000, *Accounts of Chemical Research*, 33(2), 102-110.
- Akritopoulou-Zanze, I. 2008, *Current Opinion in Chemical Biology*, 12(3), 324-331.
- Wilson, S. R. and Czarnik, A. W. 1997, John Wiley & Sons.
- Ulaczyk-Lesanko, A. and Hall, D. G. 2005, *Curr. Opin. Chem. Biol.*, 9(3), 266-276.
- Nasrollahzadeh, M. and Sajadi, S. M. 2015, *RSC Advances*, 5(57), 46240-46246.
- Sasikala, R., Rani, S. K., Easwaramoorthy, D. and Karthikeyan, K. 2015, *RSC Advances*, 5(70), 56507-56517.
- Moghaddam, F. M., Ayati, S. E., Hosseini, S. H. and Pourjavadi, A. 2015, *RSC Advances*, 5(43), 34502-34510.
- Bhuyan, D., Saikia, M. and Saikia, L. 2015, *Catalysis Communications*, 58, 158-163.
- Eagalapati, N. P., Rajack, A. and Murthy, Y. 2014, *Journal of Molecular Catalysis a: Chemical*, 381, 126-131.
- Kodicherla, B., Perumgani, P. C. and Mandapati, M. R. 2014, *Applied Organometallic Chemistry*, 28(10), 756-759.
- Cole-Hamilton, D. J. 2003, *Science*, 299(5613), 1702-1706.
- Hu, A., Yee, G. T. and Lin, W. 2005, *Journal of the American Chemical Society*, 127(36), 12486-12487.
- Lewis, L. N. 1993, *Chemical Reviews*, 93(8), 2693-2730.
- Banerjee, S. and Santra, S. 2009, *Tetrahedron Letters*, 50(18), 2037-2040.
- Schlögl, R. and Abd Hamid, S. B. 2004, *Angewandte Chemie International Edition*, 43(13), 1628-1637.
- Bell, A. T. 2003, *Science*, 299(5613), 1688-1691.
- Lu, A. H., Schmidt, W., Matoussevitch, N., Bönemann, H., Spliethoff, B., Tesche, B., Bill, E., Kiefer, W. and Schüth, F. 2004, *Angewandte Chemie*, 116(33), 4403-4406.

33. Tsang, S. C., Caps, V., Paraskevas, I., Chadwick, D. and Thompsett, D. 2004, *Angewandte Chemie*, 116(42), 5763-5767.
34. Lu, A. H., Salabas, E. E. L. and Schüth, F. 2007, *Angewandte Chemie International Edition*, 46(8), 1222-1244.
35. Polshettiwar, V. and Varma, R. S. 2010, *Green Chemistry*, 12(5), 743-754.
36. Deng, J., Mo, L. P., Zhao, F. Y., Zhang, Z. H. and Liu, S. X. 2012, *ACS Combinatorial Science*, 14(5), 335-341.
37. Lei, Z., Li, Y. and Wei, X. 2008, *Journal of Solid State Chemistry*, 181(3), 480-486.
38. Gawande, M. B., Branco, P. S. and Varma, R. S. 2013, *Chemical Society Reviews*, 42(8), 3371-3393.
39. Wang, J., Liu, X. and Feng, X. 2011, *Chemical Reviews*, 111(11), 6947-6983.
40. Dömling, A. 2002, *Current Opinion in Chemical Biology*, 6(3), 306-313.
41. Abbiati, G. and Rossi, E. 2014, *Beilstein Journal of Organic Chemistry*, 10(1), 481.
42. Villaverde, G., Corma, A., Iglesias, M. and Sánchez, F. 2012, *ACS Catalysis*, 2(3), 399-406.
43. Hemalatha, K., Madhumitha, G., Kajbafvala, A., Anupama, N., Sompalle, R. and Roopan, S. M. 2013, *Journal of Nanomaterials*, 2013, 4.
44. Wang, Y. and Xia, Y. 2004, *Nano Letters*, 4(10), 2047-2050.
45. Iravani, S. 2011, *Green Chemistry*, 13(10), 2638-2650.
46. Priyadarshana, G., Kottegoda, N., Senaratne, A., Alwis, A. D. and Karunaratne, V. 2015, *Journal of Nanomaterials*, 16(1), 317.
47. Zhou, Y., Dong, C. K., Han, L. L., Yang, J. and Du, X. W. 2016, *ACS Catalysis*, 6(10), 6699-6703.
48. Raghunandan, D., Basavaraja, S., Mahesh, B., Balaji, S., Manjunath, S. Y. and Venkataraman, A. 2009, *Nanobiotechnology*, 5(1-4), 34-41.
49. Takezawa, Y. and Imai, H. 2006, *Small*, 2(3), 390-393.
50. Moyano, D. F. and Rotello, V. M. 2011, *Langmuir*, 27(17), 10376-10385.
51. Bajpai, S., Singh, S. and Srivastava, V. 2017, *Synthetic Communications*, 47(16), 1514-1525.
52. Kidwai, M., Bansal, V., Kumar, A. and Mozumdar, S. 2007, *Green Chemistry*, 9(7), 742-745.
53. Banerjee, S. and Sereda, G. 2009, *Tetrahedron Letters*, 50(50), 6959-6962.
54. Xie, X., Liu, Z. Q., Haruta, M. and Shen, W. 2009, *Nature*, 458(7239), 746.
55. Choi, S. I., Xie, S., Shao, M., Odell, J. H., Lu, N., Peng, H. C., Protsailo, L., Guerrero, S., Park, J., Xia, X. and Wang, J., 2013, *Nano letters*, 13(7), 3420-3425.
56. Reinares-Fisac, D., Aguirre-Díaz, L. M., Iglesias, M., Snejko, N., Gutiérrez-Puebla, E., Monge, M. A. and Gándara, F. 2016, *Journal of the American Chemical Society*, 138(29), 9089-9092.
57. Gascon, J., Aktay, U., Hernandez-Alonso, M. D., van Klink, G. P. and Kapteijn, F. 2009, *Journal of Catalysis*, 261(1), 75-87.
58. Corma, A., Iborra, S., Rodriguez, I. and Sanchez, F. 2002, *Journal of Catalysis*, 211(1), 208-215.
59. Chacko, P. and Shivashankar, K. 2017, *Chinese Chemical Letters*, 28(7), 1619-1624.
60. Ghavami, M., Koohi, M. and Kassaei, M. Z. 2013, *Journal of Chemical Sciences*, 125(6), 1347-1357.
61. Zakeri, M., Abouzari-lotf, E., Miyake, M., Mehdipour-Ataei, S. and Shameli, K. 2017, *Arabian Journal of Chemistry*, <https://doi.org/10.1016/j.arabj.2017.11.006>
62. Rodriguez, I., Sastre, G., Corma, A. and Iborra, S. 1999, *Journal of Catalysis*, 183(1), 14-23.
63. Wang, Q., Wang, D. X., Wang, M. X. and Zhu, J. 2018, *Accounts of Chemical Research*, 51(5), 1290-1300.
64. Toda, F. 1995, *Accounts of Chemical Research*, 28(12), 480-486.
65. Baghery, S., Zolfigol, M. A., Schirhagl, R., Hasani, M., Stuart, M. C. and Nagl, A. 2017, *Applied Organometallic Chemistry*, 31(12), e3883.
66. Singha, S., Saha, A., Goswami, S., Dey, S. K., Payra, S., Banerjee, S., Kumar, S. and Saha, R. 2017, *Crystal Growth & Design*, 18(1), 189-199.
67. Astruc, D., Lu, F. and Aranzaes, J. R. 2005, *Angewandte Chemie International Edition*, 44(48), 7852-7872.
68. Molenbroek, A. M., Helveg, S., Topsøe, H. and Clausen, B. S. 2009, *Topics in Catalysis*, 52(10), 1303-1311.

69. Baig, R.N. and Varma, R. S. 2013, *Green Chemistry*, 15(2), 398-417.
70. Kantam, M. L., Yadav, J., Laha, S., Srinivas, P., Sreedhar, B. and Figueras, F. 2009, *The Journal of Organic Chemistry*, 74(12), 4608-4611.
71. Gharib, A., Noroozi Pesyan, N., Vojdani Fard, L. and Roshani, M. 2014, *Organic Chemistry International*, 2014, 1-6.
72. Brioché, J., Masson, G. and Zhu, J. 2010, *Organic letters*, 12(7), 1432-1435.
73. Kumar, A., Saxena, D. and Gupta, M. K. 2013, *Green Chemistry*, 15(10), 2699-2703.
74. Bazgir, A., Hosseini, G., and Ghahremanzadeh, R. 2013, *ACS Combinatorial Science*, 15(10), 530-534.
75. Ziarani, G. M., Badiei, A., Mousavi, S., Lashgari, N. and Shahbazi, A. 2012, *Chinese Journal of Catalysis*, 33(11-12), 1832-1839.
76. Tailor, Y. K., Khandelwal, S., Kumari, Y., Awasthi, K. and Kumar, M. 2015, *RSC Advances*, 5(57), 46415-46422.
77. Mouradzadegan, A., Ma'mani, L., Mahdavi, M., Rashid, Z., Shafiee, A., Foroumadi, A. and Dianat, S. 2015, *RSC Advances*, 5(101), 83530-83537.
78. Banerjee, S., Horn, A., Khatri, H. and Sereda, G. 2011, *Tetrahedron letters*, 52(16), 1878-1881.
79. Bhattacharyya, P., Pradhan, K., Paul, S. and Das, A. R. 2012, *Tetrahedron Letters*, 53(35), 4687-4691.
80. Smith, M. B. and March, J. 2007, John Wiley & Sons.
81. Duthaler, R. O. 1994, *Tetrahedron*, 50(6), 1539-1650.
82. Weinstock, L. M., Davis, P., Handelsman, B. and Tull, R. 1966, *Tetrahedron Letters*, 7(12), 1263-1268.
83. Matier, W., Owens, D. A., Comer, W. T., Deitchman, D., Ferguson, H. C., Seidehamel, R. J. and Young, J. R. 1973, *Journal of Medicinal Chemistry*, 16(8), 901-908.
84. Armstrong, R. W., Tellew, J. E. and Moran, E. J. 1992, *The Journal of Organic Chemistry*, 57(8), 2208-2211.
85. Semple, J. E., Rowley, D. C., Brunck, T. K. and Ripka, W. C. 1997, *Bioorganic & Medicinal Chemistry Letters*, 7(3), 315-320.
86. Otto, H. H. and Schirmeister, T. 1997, *Chemical Reviews*, 97(1), 133-172.
87. Abell, A. and Foulds, G. 1997, *Journal of the Chemical Society, Perkin Transactions 1*(17), 2475-2482.
88. Karimi, B. and Farhangi, E. 2013, *Advanced Synthesis & Catalysis*, 355(2-3), 508-516.
89. Fontaine, P., Chiaroni, A., Masson, G. and Zhu, J. 2008, *Organic letters*, 10(8), 1509-1512.
90. Shapiro, N. and Vigalok, A. 2008, *Angewandte Chemie*, 120(15), 2891-2894.
91. Zahoor, A. F., Thies, S. and Kazmaier, U. 2011, *Beilstein Journal of Organic Chemistry*, 7, 1299-1303.
92. Nixey, T. and Hulme, C. 2002, *Tetrahedron Letters*, 43(38), 6833-6835.
93. Doemling, A. and Illgen, K. 2005, *Synthesis*, 2005(04), 662-667.
94. Soeta, T., Kojima, Y., Ukaji, Y. and Inomata, K. *Organic letters*, 12(19), 4341-4343.
95. Basso, A., Banfi, L., Garbarino, S. and Riva, R. 2013, *Angewandte Chemie International Edition*, 52(7), 2096-2099.
96. Liu, R., Liang, X., Dong, C. and Hu, X. 2004, *Journal of the American Chemical Society*, 126(13), 4112-4113.
97. Ohnstad, H. O., Paulsen, E. B., Noordhuis, P., Berg, M., Lothe, R. A., Vassilev, L. T. and Myklebost, O. 2011, *BMC cancer*, 11(1), 1-11.
98. Shen, H. and Maki, C. G. 2010, *Journal of Biological Chemistry*, 285(30), 23105-23114.
99. Serradell, A., Herrero, R., Villanueva, J. A., Santos, J. A., Moncho, J. M. and Masdeu, J. 2003, *British Journal of Anaesthesia*, 91(4), 519-524.
100. Shepherd, J. and Ibba, M. 2013, *FEBS Letters*, 587(18), 2895-2904.
101. Genin, M. J., Allwine, D. A., Anderson, D. J., Barbachyn, M. R., Emmert, D. E., Garmon, S. A., Graber, D. R., Grega, K. C., Hester, J. B., Hutchinson, D. K. and Morris, J. 2000, *Journal of Medicinal Chemistry*, 43(5), 953-970.
102. Trost, B. M. and Brennan, M. K. 2009, *Synthesis*, 2009(18), 3003-3025.
103. Bhaskar, G., Arun, Y., Balachandran, C., Saikumar, C. and Perumal, P. T. 2012, *European Journal of Medicinal chemistry*, 51, 79-91.

104. Jiang, X., Sun, Y., Yao, J., Cao, Y., Kai, M., He, N., Zhang, X., Wang, Y. and Wang, R. 2012, *Advanced Synthesis & Catalysis*, 354(5), 917-925.
105. Galliford, C. V. and Scheidt, K. A. 2007, *Angewandte Chemie International Edition*, 46(46), 8748-8758.
106. Nair, M. and Nagarajan, K. 1983, Springer, 163-252.
107. Nawwar, G. A., Grant, N. M., Swellem, R. H. and Elseginy, S. A. 2013, *Der. Pharma. Chemica*, 5, 241-255.
108. Al-Tel, T. H. and Al-Qawasmeh, R. A. 2010, *European Journal of Medicinal Chemistry*, 45(12), 5848-5855.
109. Baviskar, A. T., Madaan, C., Preet, R., Mohapatra, P., Jain, V., Agarwal, A., Guchhait, S. K., Kundu, C. N., Banerjee, U. C. and Bharatam, P. V. 2011, *Journal of Medicinal Chemistry*, 54(14), 5013-5030.
110. Andreani, A., Granaiola, M., Leoni, A., Locatelli, A., Morigi, R., Rambaldi, M., Lenaz, G., Fato, R., Bergamini, C. and Farruggia, G. 2005, *Journal of Medicinal Chemistry*, 48(8), 3085-3089.
111. Lacerda, R. B., de Lima, C. K., da Silva, L. L., Romeiro, N. C., Miranda, A. L. P., Barreiro, E. J. and Fraga, C. A. 2009, *Bioorganic & Medicinal Chemistry*, 17(1), 74-84.
112. Gao, M., Wang, M. and Zheng, Q. H. 2014, *Bioorganic & Medicinal Chemistry Letters*, 24(1), 254-257.
113. Wallmark, B., Briving, C., Fryklund, J., Munson, K., Jackson, R., Mendlein, J., Rabon, E. and Sachs, G. 1987, *Journal of Biological Chemistry*, 262(5), 2077-2084.
114. Bonsignore, L., Loy, G., Secci, D. and Calignano, A. 1993, *European Journal of Medicinal Chemistry*, 28(6), 517-520.
115. Foye, W. 1991, *Principi di Chimico Farmaceutica Piccin*. Padova, Italy, 1991, 416.
116. Khalafi-Nezhad, A., Divar, M. and Panahi, F. 2015, *RSC Advances*, 5(3), 2223-2230.
117. Maleki, A. and Aghaei, M. 2017, *Ultrasonics Sonochemistry*, 38, 115-119.
118. Lee, J., Kim, J. and Hyeon, T. 2006, *Advanced Materials*, 18(16), 2073-2094.
119. Kim, M., Sohn, K., Na, H. B. and Hyeon, T. 2002, *Nano Letters*, 2(12), 1383-1387.
120. Abu-Reziq, R., Alper, H., Wang, D. and Post, M. L. 2006, *Journal of the American Chemical Society*, 128(15), 5279-5282.
121. Azizi, N. and Farhadi, E. 2018, *Applied Organometallic Chemistry*, 32(3), e4188.
122. Mostafavi, M. M. and Movahedi, F. 2018, *Applied Organometallic Chemistry*, 32(4), e4217.
123. Rajesh, U. C., Wang, J., Prescott, S., Tsuzuki, T. and Rawat, D. S. 2014, *ACS Sustainable Chemistry & Engineering*, 3(1), 9-18.
124. Casapullo, A., Bifulco, G., Bruno, I. and Riccio, R. 2000, *Journal of Natural Products*, 63(4), 447-451.
125. Horgen, F. D., delos Santos, D. B., Goetz, G., Sakamoto, B., Kan, Y., Nagai, H. and Scheuer, P. J. 2000, *Journal of Natural Products*, 63(1), 152-154.
126. Bailar Jr, J. 1964, *Coordination Polymers*. Prep. Inorg. React, 1.
127. Yaghi, O. M., Li, H., Davis, C., Richardson, D. and Groy, T. L. 1998, *Accounts of Chemical Research*, 31(8), 474-484.
128. Furukawa, H., Cordova, K. E., O'Keeffe, M. and Yaghi, O. M. 2013, *Science*, 341(6149), 1230444.
129. Chevreau, H., Devic, T., Salles, F., Maurin, G., Stock, N. and Serre, C. 2013, *Angewandte Chemie*, 125(19), 5160-5164.
130. McGuirk, C. M., Katz, M. J., Stern, C. L., Sarjeant, A. A., Hupp, J. T., Farha, O. K. and Mirkin, C. A. 2015, *Journal of the American Chemical Society*, 137(2), 919-925.
131. Wang, Z. and Cohen, S. M. 2009, *Chemical Society Reviews*, 38(5), 1315-1329.
132. Lee, J., Farha, O. K., Roberts, J., Scheidt, K. A., Nguyen, S. T. and Hupp, J. T. 2009, *Chemical Society Reviews*, 38(5), 1450-1459.
133. Dhakshinamoorthy, A., Alvaro, M. and Garcia, H. 2012, *Chemical communications*, 48(92), 11275-11288.
134. Azarifar, D., Ghorbani-Vaghei, R., Daliran, S. and Oveisi, A. R. 2017, *ChemCatChem*, 9(11), 1992-2000.
135. Darder, M. and Ruiz-Hitzky, E. 2005, *Journal of Materials Chemistry*, 15(35-36), 3913-3918.

-
136. Innocenzi, P. and Lebeau, B. 2005, *Journal of Materials Chemistry*, 15(35-36), 3821-3831.
 137. Bauer, F., Gläsel, H. J., Hartmann, E., Langguth, H. and Hinterwaldner, R. 2006, *International Journal of Adhesion and Adhesives*, 26(7), 567-570.
 138. Maleki, A., Ravaghi, P., Aghaei, M. and Movahed, H. 2017, *Research on Chemical Intermediates*, 43(10), 5485-5494.
 139. Maleki, A., Haji, R. F., Ghassemi, M. and Ghafuri, H. 2017, *Journal of Chemical Sciences*, 129(4), 457-462.
 140. Pu, L. and Yu, H. B. 2001, *Chemical Reviews*, 101(3), 757-824.
 141. Noyori, R. 2002, *Angewandte Chemie International Edition*, 41(12), 2008-2022.
 142. Hayashi, T. and Yamasaki, K. 2003, *Chemical Reviews*, 103(8), 2829-2844.
 143. Knowles, W. S. 2002, *Angew Chem Int Ed*, 41(12), 1998-2007.
 144. Uhm, Y. R., Lee, H. M., Olga, F., Irina, O., Marina, V., Gennady, R., Valery, C. and Rhee, C. K. 2010, *Research on Chemical Intermediates*, 36(6-7), 867-873.